Received: 26 January 2020 | Revised: 4 June 2020 | Accepted: 22 June 2020

DOI: 10.1002/2050-7038.12549

WILEY

RESEARCH ARTICLE

Sizing of underwater gravity storage with solid weights participating in electricity markets

Jean-François Toubeau[1] | **Chloé Ponsart**[1] | **Christophe Stevens**[2] | **Zacharie De Grève**[1] | **François Vallée**[1]

[1]Electrical Power Engineering Unit, Power Systems and Markets Research Group, University of Mons, Mons, Belgium

[2]SinkFloatSolutions SARL, Clermont-Ferrand, France

Correspondence
Jean-François Toubeau, Power Systems and Markets Research Group, University of Mons, Mons, Belgium.
Email: jean-francois.toubeau@umons.ac.be

Peer Review
The peer review history for this article is available at https://publons.com/publon/10.1002/2050-7038.12549.

Summary

This paper investigates the techno-economic feasibility of the innovative concept of gravity energy storage, where heavy weights are raised and lowered in a water environment. Such eco-friendly systems can be implemented in existing flooded pits or quarries, by leveraging the important depth of these cavities. Moreover, in addition to their long lifetime, they have no visual impact on the landscape, and offer a lot of flexibility to the power system. In this work, we firstly present an analytical study of the storage solution, which allows deriving tractable mathematical constraints describing its operation, such as its nonlinear speed-power curves in both charge and discharge modes. These constraints are then integrated into the investment strategy of a merchant unit that seeks to maximize its profit by jointly participating in the energy and secondary reserve markets. The model is formulated within a stochastic framework to ensure robustness of sizing decisions in view of future market uncertainties. Results from a practical case study (on a natural cavity of 200 m) show that underwater gravity storage is a cost-efficient technology that offers payback periods of less than 10 years, mainly due to its intrinsic low capital costs estimated at around 100 €/kWh.

List of Symbols and Abbreviations: $\bar{n}^{\text{blocks}}$, Number of installed blocks; $\bar{n}^{\text{gm}}$, Number of installed geared induction machines; φ^{CAPEX}, Total investment costs of the storage system, €; $\varphi^{\text{OPEX}}_{\omega,t}$, Total profit from storage operation in scenario ω at time t, €; $n^{\text{blocks}}_{\omega,t}$, Number of blocks stored within the storage system in scenario ω at time t; $p^{\text{dis,res}}_{\omega,t}, p^{\text{ch,res}}_{\omega,t}$, Actual output power in discharge (dis) and charge (ch) modes after the real-time activation of reserves in scenario ω at time t, MW; $p^{\text{dis}}_{\omega,t}, p^{\text{ch}}_{\omega,t}$, Output power in discharge (dis) and charge (ch) modes committed in the energy market in scenario ω at time t, MW; $p^{\text{single,}\cdot\text{,res}}_{\omega,t}$, Output power per induction machine in discharge (dis) and charge (ch) modes after the real-time activation of reserves in scenario ω at time t, MW; $res^{\text{dis}}_{\omega,t}, res^{\text{ch}}_{\omega,t}$, Reserve capacity allocated in the upward secondary reserve market in discharge (dis) and charge (ch) mode in scenario ω at time t, MW; $v^{\text{dis}}_{\omega,t}, v^{\text{ch}}_{\omega,t}$, Aggregated block speed (at the UGES level) in discharge (dis) and charge (ch) mode in scenario ω at time t, m/s; $v^{\text{single,}\cdot}_{\omega,t}$, Block speed per induction machine in discharge (dis) and charge (ch) mode in scenario ω at time t, m/s; $z^{\text{dis}}_{\omega,t}, z^{\text{ch}}_{\omega,t}$, Binary variables indicating the discharge (dis) and charge (ch) status in scenario ω at time t; Δ_t, Optimization step, 1 hour; $\eta^{\text{dis}}, \eta^{\text{ch}}$, Efficiency of the storage system in discharge (dis) and charge (ch) modes; $\kappa_{\omega,t} \in [0,1]$, Activation rate of the upward reserve; $\lambda^{\text{act}}_{\omega,t}$, Price for activation of balancing reserves in scenario ω at time t, €/MWh; $\lambda^{\text{EN}}_{\omega,t}$, Electricity price in the energy-only market in scenario ω at time t, €/MWh; $\lambda^{\text{res}}_{\omega,t}$, Price for availability of reserve capacity in scenario ω at time t, €/MW; $\bar{N}^{\text{gm}}$, Maximum number of blocks that can be installed, based on the site topology; $\bar{P}^{\text{dis}}, \bar{P}^{\text{ch}}$, Maximum power rating in discharge (dis) and charge modes, MW; $\pi_{\omega,\,t}$, Probability of occurrence of scenario ω; D, Depth of the water cavity, m; $M^{\text{dis}}, M^{\text{ch}}$, Large positive constants; $MC^{\text{dis}}, MC^{\text{ch}}$, Operating costs in discharge (dis) and charge (ch) modes, €/MWh.

J.-F. Toubeau is a post-doctoral research fellow of the National Fund of Scientific Research (FNRS) at the Electrical Power Engineering Unit, University of Mons, Belgium.

Christophe Stevens is the founder and CEO of SinkFloatSolutions, technology developed and patented on several innovative mechanical processes aimed at dividing by a 10-fold ratio the cost of energy storage.

C. Ponsart, Z. De Grève and F. Vallée are with the Electrical Power Engineering Unit, University of Mons, Belgium.

KEYWORDS
electricity markets, gravity energy storage, stochastic optimization, suspended weights

1 | INTRODUCTION

With the objective to cost-effectively integrate high shares of stochastic electricity generation (mainly wind and photovoltaic) in modern power systems, new flexible solutions are currently emerging.[1,2] In particular, new concepts of gravity energy storage (GES) are coming to light, whose basic principle is to store energy under the form of gravitational potential energy. Gravity-based storage is often associated with pumped hydro energy storage (PHES), an effective solution that currently covers more than 95% of worldwide capacity.[3] The same principle can be applied with fewer constraints using a simple (easy to implement) and environment-friendly mechanical system, consisting in lifting a weight that thereby acquires potential energy, which can thereafter be released so that the kinetic energy is converted back into electrical power. Interestingly, a study from the Imperial College London Consultants[4] shows that this type of solution is currently the most cost-effective technology for bulk electricity storage, followed by pumped hydro storage (PHES) and compressed air energy storage (CAES), while battery systems still remain significantly more expensive. This mainly arises from the low capital costs of gravity storage that does not rely on costly material and has no expenses related to civil works.[5]

Overall, gravity storage has a moderate energy density (although around four times higher than PHES depending on the density of the weights), but combines multiple advantages including a continuous operation range with high ramp rates, no cycle-limit and a long lifetime during which the defective components can be easily and cost-effectively replaced.[6] This concept has thus the potential to complement current technologies. In that respect, batteries are more suited for applications involving space and weight limitations such as electric vehicles, but they are still costly and composed of polluting and non-recyclable materials for a lifetime that does not exceed 20 years.[7] For their part, PHES systems may have a negative influence on ecosystems, and are highly constrained since they require particular topographies with an important height difference between two large reservoirs.[8] To a lesser extent, compressed air technologies also need specific geographic conditions since salt caverns offer a more economical alternative than large aboveground containers (with a strong visual impact). Then, CAES have a relatively high environmental impact as they require to be linked to a gas turbine plant, for efficiencies around 50% arising from the (bidirectional) conversion between energy and pressurized gas.[9]

In this context, a Swiss startup (EnergyVault) has recently launched a 4 MW-35 MWh aboveground demonstration plant, characterized by a six-armed crane that is moving concrete blocks of 35 tons along a vertical distance of 120 m.[10] In August 2019, EnergyVault has raised $110 million from SoftBank Vision Fund to further develop the technology. In the same trend, other concepts are appearing, among which (a) EarthPumpStore where large containers filled with compacted earth materials (such as coal dust, or other waste materials) are vertically shifted within an opencast structure,[11] (b) ARES (Advanced Rail Energy Storage) which proposes shuttle-trains with axle-drive motors to transport masses up- and down-hill to respectively store and generate electricity,[12] or (c) Gravitricity that exploits abandoned mine shaft for raising and lowering a heavy weight.[13]

In this paper, which results from a collaborative research between university and industry (SinkFloatSolutions[14]), we examine the techno-economic feasibility of underwater gravity energy storage (UGES). The innovative system is operating in water through the exploitation of existing underground cavities, such as end-of-life flooded quarries, in which heavy blocks (typically between 5 and 50 tons) are moved between the bottom and the surface of the water. The potential of such sites typically varies between 1 and 10 MW (for a few hours duration) for medium-sized water cavities (depth of 200-300 m). Compared to the EnergyVault system, this solution does not rely on cranes (thus considerably reducing investment costs), and has no visual impact on the environment. Moreover, the UGES operation is more stable since it is not influenced by bad weather conditions such as high winds. However, the techno-economic feasibility of the UGES system still needs to be properly evaluated. In that regard, this work aims to provide a technical study of this new solution. The results are then leveraged to conduct a economic analysis based on the performance of a representative case study. Such a global study is an important milestone for considering whether further research is justified, and to attract investment in potential projects. Overall, the contributions of this work are 3-fold.

Firstly, we perform an analytical study of the UGES operation in both charge and discharge. Interestingly, we show that transient effects (to accelerate the block from idle mode to full power) become marginal after 15 seconds, so that the system can provide both primary and secondary reserve (response time of respectively 30 seconds and 7.5 minutes) without oversizing the electric machine and the associated power electronics converters. Moreover, this analysis also enables to derive a mathematical

model describing the UGES operation. In particular, we extract the UGES efficiency curves, which characterize the nonlinear relationship (arising from the fluid resistance) between the output power (in MW) and the block speed (in m/s).

Secondly, the UGES operating constraints are incorporated into the sizing procedure, which aims at determining the optimal UGES power and energy ratings in order to maximize the system value over its expected lifetime. The optimization is formulated as a mixed-integer linear program, by replacing the nonlinear dependencies by tractable piecewise linear approximations. Practically, the UGES maximizes its profit by jointly participating to (a) energy arbitrage (ie, discharging electricity at high peak prices and charging during low off-peak prices[15]) and (b) the provision of operating reserves (ie, power capacity offered in day-ahead to the system operator that can be activated in real-time to maintain the system frequency), within the competitive framework of European electricity markets.[16,17]

Thirdly, we analyze the robustness of the sizing solution for different risk attitudes, by adjusting the discount rate on the investment model. We thereby study the trade-off between the size of the storage unit and the resulting profit that can be leveraged in electricity markets. Results from a practical case study show that UGES is a competitive solution (with attractive return on investments), which combines the advantages of low investment and operation costs, and high flexibility (allowing to efficiently mutualize revenues streams in energy and reserve markets). Such outcomes provide evidence of the economic viability of the solution, and support the interest for further technology developments and demonstrations.

The rest of the paper is structured as follows. In Section 2, we explain the characteristics and design of the proposed underwater GES solution. An analytical study of the UGES operation is carried out in Section 3, which provides input information for the investment procedure, which is formulated in Section 4. A case study investigating the investment decisions in different conditions is presented in Section 5. Finally, the work is concluded in Section 6.

2 | WORKING PRINCIPLE OF THE STORAGE SYSTEM

Figure 1 depicts the main components of the proposed UGES technology. The system consists of a number of solid blocks, which are stored using flotation devices. Each block can be connected to an induction machine (via a winch) that can alternatively lower the weight for producing electricity, and then lift it back to store potential energy. A mobile waterproof platform (containing the electromechanical system) can be moved from one block to the next, and the blocks are then hooked (and unhooked) to the system via an automated robot.

The speed of the induction machine is controlled via a variable-frequency drive, which enables its operation over a large output power range without loss of efficiency. This moreover provides a bidirectional interface with the electrical network, that is, the machine operates as a motor when charging and as a generator during discharge. Since the winch needs to rotate at a much lower speed than the motor, both systems are connected via a R:1 speed reduction gear. As further described in Section 3, this gearbox has also the positive effect of decreasing the motor torque, and thus its volume and price.

For avoiding downtimes (ensure continuity of the output power), two electromechanical systems (ie, from power electronics to the winch) operating independently are needed. For instance, in discharge mode, when one block moves downwards, the other system will hook a new weight that can then be released when the first one hits the cavity bottom.

Interestingly, the UGES solution allows to decouple the power rating from its energy capacity. The output power (in MW) is defined by the weight of the blocks, and the number of induction machines operating in

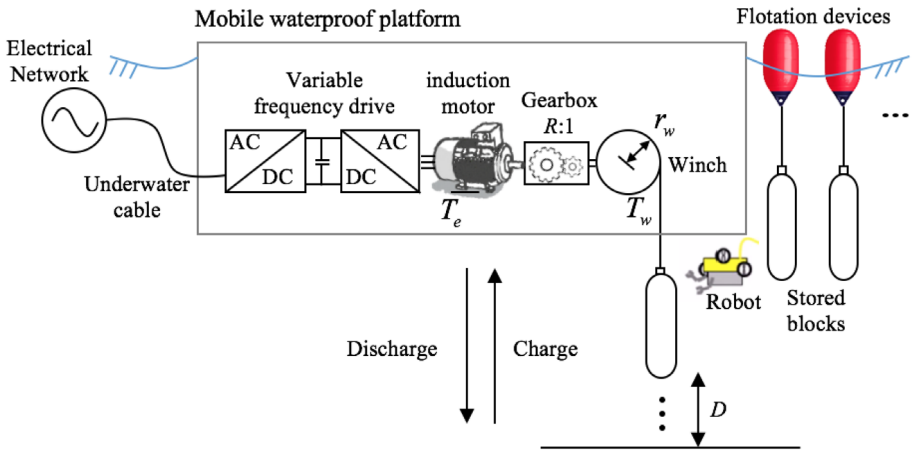

FIGURE 1 Typical conversion chain (for a single electromechanical system) of an underwater gravity energy storage (UGES) system

parallel (ie, each variable frequency drive can be connected to several machines to multiply the number of blocks that can be simultaneously moved). The UGES energy capacity (in MWh) is reflected by the total number of blocks.

Overall, it should be noted that the practical feasibility of the UGES solution is constrained by its ability to capture a new block before the previous one ends its travel. This constraint is directly linked to the depth of the cavity, since larger heights offer more time to perform the hooking operation. In case of problem, investors may also investigate the potential of relying on a third electromechanical system. In parallel, the intense use constraints on the geared induction machine (due to the very frequent start-up and shut-down) is a key element to consider in the sizing procedure.

3 | ANALYTICAL STUDY OF THE STORAGE SYSTEM

This section analyses the UGES operating conditions, with the aim of providing an analytical description of the power, energy and ramp rates in both charge and discharge modes.

3.1 | Efficiency curves

The system operation is studied through the equation of motion on the drive (connecting the induction motor and the gearbox). It should be noted that the weight of the wire rope is neglected, that is, small in comparison to the weight of the block.[13,18] Hence, the torque T_e of the electrical machine needed to counterbalance the load torque T_w, taking inertia effects into account, is given by:

$$\eta T_e = \frac{T_w}{R} + J_e \frac{\mathrm{d}\omega}{\mathrm{d}t} = \frac{F_w r_w}{R} + J_e \frac{aR}{r_w}, \tag{1}$$

where η is the global efficiency of the installation, r_w is the winch radius, and $a = \mathrm{d}v/\mathrm{d}t$ is the block acceleration. The block speed v is linked to the rotational speed of the motor $\omega = vR/r_w$ through the gear ratio R. The equivalent moment of inertia of the system J_e (referred to the electrical machine shaft) include contributions from the electrical machine, the gearbox and the load.[19]

$$J_e = J_m + \frac{J_g}{R^2} + m\left(\frac{r_w}{R}\right)^2, \tag{2}$$

where J_e is the moment of inertia of the geared electric machine, in which J_m and J_g are respectively the moments of inertia of the machine and the gearbox.

The force F_w applied on the underwater block results from three contributions, which differs when the block is lifted (in charge) and lowered (in discharge). Two effects are insensitive to the motion direction, that is, . (a) the block weight, and (b) the buoyant force (due to Archimedes' principle), while (c) the fluid resistance (or drag force) opposes movement. Hence, the resultant forces in charge (3) and discharge (4) are cast as:

$$F^{\mathrm{ch}} = \underbrace{mg}_{\text{(i)}} - \underbrace{\rho_{\mathrm{water}} V g}_{\text{(ii)}} + \underbrace{0.5 C_T(ge, Re)\rho_{\mathrm{water}} v^2 S_{\mathrm{ref}}}_{\text{(iii)}} \tag{3}$$

$$F^{\mathrm{dis}} = \underbrace{mg}_{\text{(i)}} - \underbrace{\rho_{\mathrm{water}} V g}_{\text{(ii)}} - \underbrace{0.5 C_T(ge, Re)\rho_{\mathrm{water}} v^2 S_{\mathrm{ref}}}_{\text{(iii)}}, \tag{4}$$

where g is the gravity (9.81 m/s^2), ρ_{water} is the water density (1000 kg/m^3), and m is the block mass (in kg), V its volume (in m^3), and S_{ref} its cross sectional area (in m^2, which depends on its shape). The drag coefficient C_T varies with the block geometry (ge) and the Reynolds number (Re). A lower bound of Re is estimated in Equation (5), where L is a characteristic linear dimension (m), and μ is the fluid kinematic viscosity (m^2/s):

$$Re = \frac{vL}{\mu} = \frac{1 \times 1}{1.007 \times 10^{-6}} \approx 10^6. \tag{5}$$

The low kinematic viscosity of the water (about 17 times lower than the air) and the large dimension of the block (above 1 m) result in high Reynold numbers ($>10^6$ for typical speeds $v > 1$ m/s). Interestingly, such values of Re correspond to a stable behavior of the fluid resistance,[20] so that C_T can be considered as a constant parameter in our application.

By respectively inserting Equations (3) and (4) into the torque equation (1), and by using $p = T_e\omega$, with $\omega > 0$ in charge mode (by convention), we obtain the output power of the electrical machine in both charge p^{ch} and discharge p^{dis} modes:

$$\eta^{\text{ch}} p^{\text{ch}} = \underbrace{(mg - \rho_{\text{water}} Vg)v + (0.5 C_T \rho_{\text{water}} S_{\text{ref}})v^3}_{p_{SS}^{\text{ch}}} + \left(m + \frac{J_e}{(r_w \omega)^2}\right) va \tag{6}$$

$$\frac{1}{\eta^{\text{dis}}} p^{\text{dis}} = \underbrace{(mg - \rho_{\text{water}} Vg)v - (0.5 C_T \rho_{\text{water}} S_{\text{ref}})v^3}_{p_{SS}^{\text{dis}}} - \left(m + \frac{J_e}{(r_w \omega)^2}\right) va. \tag{7}$$

In this work, we consider blocks of steel slag (a waste material coming from the process of steel making), which combines the advantages of high density (3500 kg/m^3), small price (0.02 €/kg), and the possibility to be agglomerated within inert (clean) barrels with a good aerodynamic shape ($C_T = 0.84$). The efficiencies in charge η^{ch} and discharge η^{dis} are estimated at 0.95 (round-trip efficiency of around 0.9), and come from losses in both electric components (variable-speed drive and geared induction machine), and the mechanical part (friction in the winch). Hence, in steady-state conditions, the efficiency curves (6) and (7) linking the output power (p_{SS}^{ch} in charge and p_{SS}^{dis} in discharge) and the block speed v are depicted in Figure 2 for different block weights.

It can be seen that increasing the power to lift the block monotonically augments its speed. The discharge power p_{SS}^{dis} theoretically follows a bell curve, where the power extracted from the block's fall increases with the speed until a threshold value $\bar{v}^{\text{dis}}$. At that point, the optimal trade-off in steady-state conditions is achieved in Equation (7) between the forces with a positive contribution (which are proportional to v), that is, block weight minus buoyant force, and the negative drag force (proportional to v^3). In the following, blocks of 25 tons, that is, . $V = 7.14$ m^3 (with $S_{\text{ref}} = 1.7$ m^2) will be used (Figure 3).

3.2 | Energy-to-power ratio

From the efficiency curves, it can be inferred that the UGES energy capacity e is not fixed, but depends on the operational power profile and the total number of blocks $\bar{n}^{\text{blocks}}$.

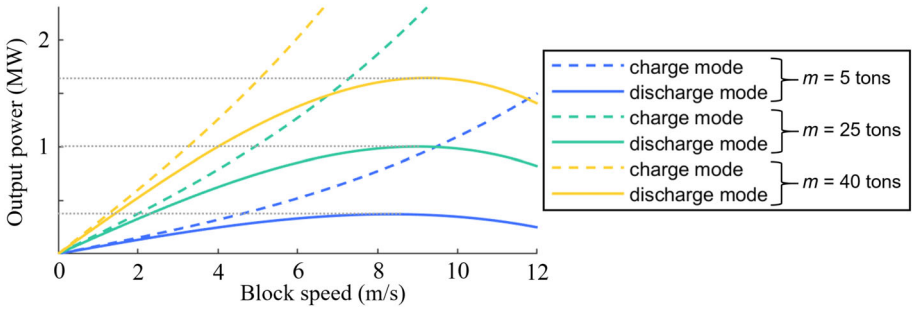

FIGURE 2 Efficiency curves between the output power and block's speed in both charge and discharge

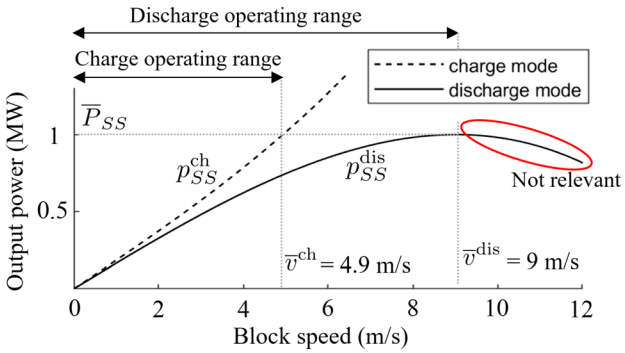

FIGURE 3 Efficiency curves between the output power and block's speed in both charge and discharge

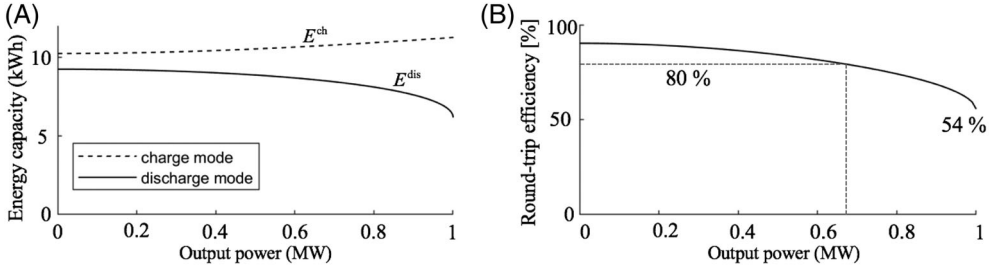

FIGURE 4 Efficiency characteristics of the UGES technology, with A, the energy to power ratio in both charge and discharge modes, and B, the resulting round-trip efficiency

$$e = p \cdot \Delta t \cdot \bar{n}^{\text{blocks}} = p \cdot \frac{D}{3600 \cdot v} \cdot \bar{n}^{\text{blocks}}, \tag{8}$$

where Δt is the time (in hours) to move one block along the depth ($D = 200$ m) of the cavity. The power to energy relation (for a single block $\bar{n}^{\text{blocks}} = 1$) is shown in Figure 4A. Due to losses in the conversion chain, the energy that can be stored by the system is higher than the energy that can be supplied back to the grid. However, this difference is nonlinear in UGES due to the additional contribution of the fluid resistance (which is proportional to v^3). In that regard, an energy of 9.2 kWh can be generated when lowering one block of 25 tons at low speed, but this capacity is reduced to 6.2 kWh when generating at maximum power (1 MW during a descent of 22.2 seconds). In charge, the effect of fluid resistance is less important, and the stored energy (for one block) varies from 10.2 kWh at low speed, up to 11.3 kWh at maximum speed (4.9 m/s). The resulting impact on the UGES round-trip efficiency (ie, fraction of energy put into the storage system that can be retrieved) is shown in Figure 4B, where we observe that the UGES performance strongly depends on the operating conditions. Interestingly, the UGES efficiency is higher than 80% for operation levels below two-third of the maximum rated power $\bar{P}_{SS} = 1$ MW, but it then decreases (down to 54%) under high-power output characteristics. This effect is represented in Equations (6) and (7), and can be alleviated by reducing (a) the drag coefficient C_T of the blocks (through an improved aerodynamic shape), and (b) their cross-sectional area S_{ref}.

3.3 | Sizing of motor and power electronics

For an investor, efficiency curves (Figure 3) are essential to properly size the UGES components. In that respect, for a typical four-pole motor, the full load speed is around 1450 rotations per minute (rotor slip of around 3% on the 50 Hz European grid). Given that on the maximum block speed is achieved at $\bar{v}^{\text{dis}} = 9$ m/s, the gear ratio between the winch (with a radius $r_w = 1$ m) and the motor can be computed as:

$$R = \omega \frac{r_w}{\bar{v}^{\text{dis}}} = \frac{1450 \times 2\pi}{60} \frac{1}{9} = 16.9. \tag{9}$$

The speed of the electrical machine (between zero and its full speed) is then more finely controlled via a variable-frequency drive (VFD).

In addition, efficiency curves (Figure 3) also show that the maximum steady-state generation power is equal to $\bar{P}_{SS} = 1\,\text{MW}$. However, if the UGES aims at providing fast frequency response, one should account for the additional power (with respect to steady-state conditions) that is required for accelerating the block. By assuming a constant acceleration a, the transient power rating p^{ch} to reach the speed v^{ch} (from idle state $v^{\text{ch}} = 0\,\text{m/s}$) in a response time τ (s) is given by

$$\begin{aligned}\eta^{\text{ch}} p^{\text{ch}} &= p_{SS}^{\text{ch}} + \frac{1}{\tau}\left(m + \frac{J_e}{(r_w R)^2}\right)\left(v^{\text{ch}}\right)^2 \\ &= p_{SS}^{\text{ch}} + \frac{1}{\tau}\left(m + \frac{J_e}{(r_w R)^2}\right) \\ &\quad \left(\frac{p_{SS}^{\text{ch}}}{mg - \rho_{\text{water}} V g - 0.5 C_T \rho_{\text{water}} v^2 S_{\text{ref}}}\right)^2 .\end{aligned} \tag{10}$$

Using Equation (10) with a moment of inertia J_e of 100 kg. m^2 (typical value for medium voltage geared motor[21]), we evaluate the additional power required to achieve a given response time τ. Outcomes are represented in Figure 5, where it is observed that the transient contribution is prominent for faster ramp rates (especially for achieving higher power), with a power around $p^{\text{ch}} = 1.9\bar{P}_{SS}$ to reach the maximum speed $\bar{v}^{\text{ch}} = 4.9\,\text{m/s}$ in $\tau = 1\,\text{s}$. For dynamics related to primary (30 seconds) or secondary reserves (7.5 minutes), transient effects have a minor contribution (power increase of respectively 3% and 0.2%), and thereby have a marginal impact on the sizing of the electric machine and power electronics. Interestingly, we also see that the inertia contributions associated with the load $m = 25000$ kg and the motor $J_e/(r_w R)^2 \approx 31000$ kg are of the same order of magnitude, which contributes to the stable control of the system.[22]

However, in order to ensure both continuity and quality of the power supply during the transition between two blocks, it is important to efficiently coordinate the two electromechanical systems. For instance, it is possible to implement an optimized operation control scheme where a new block is accelerated during the deceleration phase of the previous one.

4 | INVESTMENT MODEL

Below, we formulate the UGES sizing problem, which consists in identifying the optimal power and energy ratings of the system in order to achieve the best trade-off between investment costs and operating profits over the planning horizon. The operating profits are leveraged through a joint participation in energy and reserve markets. The market structure is inspired by the European framework in which the energy-only and reserve capacity are cleared in day-ahead (for the 24 hours of the next day) through independent auctions. We consider that both market floors have an hourly time resolution. In this work, we focus on the secondary reserve (which is offered in day-ahead to the system operator, and that can be deployed in real-time within a timeframe of 7.5 minutes to alleviate frequency deviations) since it proved to be the most important income source.[23,24] In most European countries (such as Belgium, Denmark, etc.), the secondary reserve is paid for both capacity procurement and real-time activation. The revenues from reserve activation (at the balancing stage) are highly profitable for storage units. Indeed, the associated prices are designed to cover the

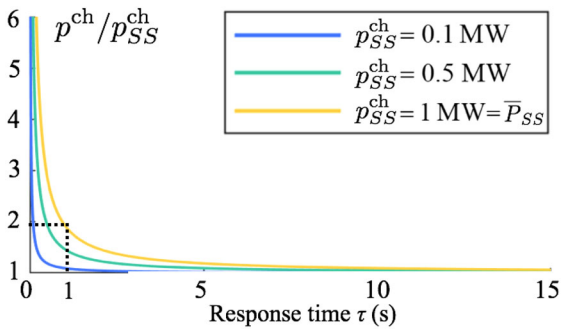

FIGURE 5 Ratio between the maximum transient power and the steady state power to achieve a desired ramp-rate

operating costs of all reserve providers through a marginal pricing (ie, the price is set by the marginally accepted offer). In the current energy mix, most of the reserve is delivered by conventional power plants which have high marginal costs compared to the UGES technology. Consequently, the price of reserve activation far exceeds the UGES operating costs, thereby providing a significant margin of profit to UGES units[25,26] (in addition to the profit leveraged from the offered capacity). In this paper, we assume that only upward reserve is provided by UGES since downward reserve can usually be more efficiently provided by rival conventional power plants due to their substantial cost savings (mainly arising from the fuel that has not been used[26-28]). It should be noted that this assumption is strongly dependent on the market conditions (ie, the prices in the different market floors and the generation mix of the studied area), but it is adequate for the Belgian case study considered in this work.

The UGES operational strategy is subject to two main sources of uncertainties. Firstly, secondary reserves can be either fully, partially or not called in real-time (depending on the grid needs), which impacts the UGES energy content and thus its operation policy.[29] Secondly, the UGES profitability is influenced by future (energy and secondary reserve) prices. To ensure risk-aware decisions, the problem is thus formulated as a stochastic program, which consists of three stages:

- investment decisions;
- daily participation in day-ahead energy and secondary reserve capacity markets;
- real-time power adjustment due to the reserve activation.

In this work, we assume that the UGES operator provides a feasible schedule, that is, it does not willingly incur imbalance penalties.[30] This allows internalizing the day-ahead and real-time steps into a single stage, such that the investment problem can be expressed as a two-stage stochastic program (Figure 6). Practically, the investor takes sizing decisions in view of future uncertainties in market conditions (represented through scenarios $\omega \in \Omega$). At the second stage, for each realization of ω, the UGES optimizes its operation over the planning horizon. This second-stage can thus be viewed as an optimization problem (in which the uncertain information is revealed), thereby describing the supposedly optimal UGES behavior in short-term markets.

In order to jointly consider the one-time capital costs and the continuous operating profits (over the UGES lifetime) on a consistent basis, all cash inflow/outflow are discounted back to their present value. All terms are then summed up to obtain the net present value (NPV) of the investment project, which allows to properly account for the inflation of capital costs and deflation of future revenues. The objective function (11) maximizes the UGES net present value, that is, its (actualized) expected profits in electricity markets minus the capital expenditures.

$$\mathrm{NPV} = -\varphi^{\mathrm{CAPEX}} + \sum_{\omega \in \Omega} \pi_{\omega} \cdot \sum_{i=1}^{N_y} \frac{\left[\sum_{t \in \mathcal{T}} \varphi_{\omega,t}^{\mathrm{OPEX}}\right]}{(1+r)^i}, \tag{11}$$

where $t \in \mathcal{T}$ are the hourly time periods within a year, r is the discount rate, and N_y is the UGES expected lifetime (in years). Here, the life of the gravity storage system is considered to be $N_y = 30$ years, with a conservative discount rate $r = 9\%$. However, since the long UGES lifetime makes it very sensitive to the interest rate (since higher discount rates

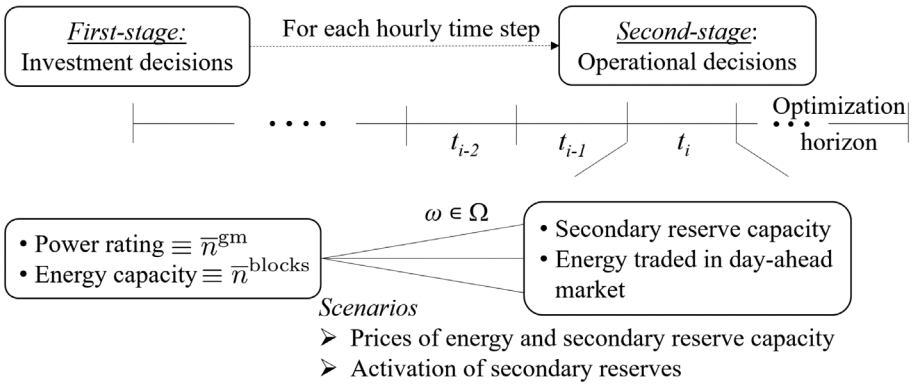

FIGURE 6 Two-stage stochastic investment model

result in lower present values), a sensitivity analysis on the impact of r on the unit profitability is carried out in Section 5.2.

The capital expenditures φ^{CAPEX} include the costs related to (a) the number of installed blocks $\bar{n}^{\mathrm{blocks}}$, (b) fixed miscellaneous fees c^{mis} (for the platform, mooring cables, etc.), and (c) the number of geared induction machines $\bar{n}^{\mathrm{gm}}$ (to which are associated a winch and a traction cable). The latter term is multiplied by a factor 2 to reflect that 2 systems are needed to enable the UGES continuous operation (Section 2).

$$\varphi^{\mathrm{CAPEX}} = \bar{n}^{\mathrm{blocks}} c^{\mathrm{blocks}} + c^{\mathrm{mis}} + 2\bar{n}^{\mathrm{gm}} \left(c^{\mathrm{gm}} + c^{\mathrm{winch}} + c^{\mathrm{cable}} \right). \tag{12}$$

The operating profit $\varphi^{\mathrm{OPEX}}_{\omega,t}$ comes from arbitrage in energy market (lines 1 and 2), procurement of upward secondary reserve capacity (line 3), and balancing revenues from the real-time activation of procured reserves (lines 4 and 5). The uncertainty in the balancing actions is modeled through scenarios of reserve activation $\kappa_{\omega,\,t} \in [0, 1]$.

$$\begin{aligned} \varphi^{\mathrm{OPEX}}_{\omega,t} = \; & \Delta_t \left(\lambda^{\mathrm{EN}}_{\omega,t} - MC^{\mathrm{dis}} \right) p^{\mathrm{dis}}_{\omega,t} \\ & - \Delta_t \left(\lambda^{\mathrm{EN}}_{\omega,t} + MC^{\mathrm{ch}} \right) p^{\mathrm{ch}}_{\omega,t} \\ & + \lambda^{\mathrm{res}}_{\omega,t} \left(res^{\mathrm{dis}}_{\omega,t} + res^{\mathrm{ch}}_{\omega,t} \right) \\ & + \Delta_t \left(\lambda^{\mathrm{act}}_{t} - MC^{\mathrm{dis}} \right) \kappa_{\omega,t} \cdot res^{\mathrm{dis}}_{\omega,t} \\ & + \Delta_t \left(\lambda^{\mathrm{act}}_{t} + MC^{\mathrm{ch}} \right) \kappa_{\omega,t} \cdot res^{\mathrm{ch}}_{\omega,t} \;\; \forall \omega, t \end{aligned} . \tag{13}$$

Constraints (14) and (15) respectively limit the number of geared induction machines $\bar{n}^{\mathrm{gm}}$ that can operate in parallel and the number of blocks $\bar{n}^{\mathrm{blocks}}$ that can be installed (reflecting topological and budget limits). Constraint (16) allows for three independent operating modes, that is, charge, discharge and idle.

$$0 \le \bar{n}^{\mathrm{gm}} \le \bar{N}^{\mathrm{gm}} \tag{14}$$

$$0 \le \bar{n}^{\mathrm{blocks}} \le \bar{N}^{\mathrm{blocks}} \tag{15}$$

$$z^{\mathrm{dis}}_{\omega,t} + z^{\mathrm{ch}}_{\omega,t} \le 1 \;\; \forall \omega, t \tag{16}$$

This UGES power schedule in both charge (17)-(19) and discharge (20)-(22) modes is constrained by the size and number of induction machines. Moreover, the power cannot be simultaneously allocated to provide both energy arbitrage and reserves (ie, the activation of the scheduled reserve capacity must be always guaranteed).

$$0 \le p^{\mathrm{ch}}_{\omega,t} \le z^{\mathrm{ch}}_{\omega,t} M^{\mathrm{ch}} \;\; \forall \omega, t \tag{17}$$

$$p^{\mathrm{ch}}_{\omega,t} \le \bar{n}^{\mathrm{gm}} \bar{P}^{\mathrm{ch}} \;\; \forall \omega, t \tag{18}$$

$$0 \le res^{\mathrm{ch}}_{\omega,t} \le p^{\mathrm{ch}}_{\omega,t} \;\; \forall \omega, t \tag{19}$$

$$0 \le p^{\mathrm{dis}}_{\omega,t} \le z^{\mathrm{dis}}_{\omega,t} M^{\mathrm{dis}} \;\; \forall \omega, t \tag{20}$$

$$0 \le res^{\mathrm{dis}}_{\omega,t} \le z^{\mathrm{dis}}_{\omega,t} M^{\mathrm{dis}} \;\; \forall \omega, t \tag{21}$$

$$p^{\mathrm{dis}}_{\omega,t} + res^{\mathrm{dis}}_{\omega,t} \le \bar{n}^{\mathrm{gm}} \bar{P}^{\mathrm{dis}} \;\; \forall \omega, t. \tag{22}$$

For the reserve market, the UGES needs to have enough stored energy, to be available in any case. To that end, it is necessary to take into consideration the impact of the (uncertain) activation of reserve in real-time, which is modeled

through different scenarios (23) and (24). For each scenario, the UGES energy content, that is, number of blocks stored at the end of each time step t, is computed in Equation (25). To that end, we model in Equation (26) the nonlinear functions f^{dis} and f^{ch} between the actual power and the block speed (depicted in Figure 3). However, the relation is modeled for a single induction machine. If the UGES invests in more induction machines $\bar{n}^{\text{gm}}$, the number of blocks that can be simultaneously moved will increase accordingly, such that the power output $p_{\omega,t}^{\text{single},\cdot,\text{res}}$ (and speed $v_{\omega,t}^{\text{single},\cdot}$) of each individual block will decrease. This will ultimately increase the operating efficiency of the whole system. This effect is captured in Equations (27) and (28), which leads to a bilinear term (through the product of a binary $\bar{n}^{\text{gm}}$ and a continuous variable), which may be easily linearized by replacing the equalities by a set of three inequalities with a big-M approach.[31]

$$p_{\omega,t}^{\text{dis,res}} = p_{\omega,t}^{\text{dis}} + \kappa_{\omega,t} \cdot res_{\omega,t}^{\text{dis}} \ \forall \omega, t \tag{23}$$

$$p_{\omega,t}^{\text{ch,res}} = p_{\omega,t}^{\text{ch}} - \kappa_{\omega,t} \cdot res_{\omega,t}^{\text{ch}} \ \forall \omega, t \tag{24}$$

$$n_{\omega,t}^{\text{blocks}} = n_{\omega,t-1}^{\text{blocks}} + \frac{3600 v_{\omega,t}^{\text{ch}}}{D} - \frac{3600 v_{\omega,t}^{\text{dis}}}{D} \ \forall \omega, t \tag{25}$$

$$p_{\omega,t}^{\text{single,dis,res}} = f^{\text{dis}}\left(v_{\omega,t}^{\text{single,dis}}\right),\ p_{\omega,t}^{\text{single,ch,res}} = f^{\text{ch}}\left(v_{\omega,t}^{\text{single,ch}}\right) \ \forall \omega, t \tag{26}$$

$$p_{\omega,t}^{\text{dis,res}} = \bar{n}^{\text{gm}} \cdot p_{\omega,t}^{\text{single,dis,res}},\ p_{\omega,t}^{\text{ch,res}} = \bar{n}^{\text{gm}} \cdot p_{\omega,t}^{\text{single,ch,res}} \ \forall \omega, t \tag{27}$$

$$v_{\omega,t}^{\text{dis}} = \bar{n}^{\text{gm}} \cdot v_{\omega,t}^{\text{single,dis}},\ v_{\omega,t}^{\text{ch}} = \bar{n}^{\text{gm}} \cdot v_{\omega,t}^{\text{single,ch}} \ \forall \omega, t. \tag{28}$$

The number of stored blocks is limited by the investment decision $\bar{n}^{\text{blocks}}$ (29). A cyclical boundary condition which equals the value of the energy content at the start and end of the optimization is imposed in Equation (30).

$$0 \le n_{\omega,t}^{\text{blocks}} \le \bar{n}^{\text{blocks}} \ \forall \omega, t \tag{29}$$

$$n_{\omega,t=T}^{\text{blocks}} \ge n_{\omega,t=0}^{\text{blocks}} = \frac{\bar{n}^{\text{blocks}}}{2} \ \forall \omega, t. \tag{30}$$

To reach a compromise between model accuracy and formulation tractability, the non-linear power curves (26) are replaced by their piecewise linear approximations. To that end, the allowed speed range $[0, \bar{v}]$ (in both charge and discharge) is partitioned into M subintervals, whose break points are:

$$\begin{pmatrix} 0 = V_0 < V_1 < \ldots < V_M = \bar{v} \\ P_m = f_j\left(V_j\right)\ j = 0, 1, \ldots, M \end{pmatrix}. \tag{31}$$

From this, the linear interpolation of $p_{\omega,t}^{\text{single,ch,res}}$ (or $p_{\omega,t}^{\text{single,dis,res}}$) of Equation (26) can then be determined, at the expense of introducing an additional set of M binary z_m^v and M continuous v_m decision variables, with the following set of equations[32]:

$$z_m^v \in \{0, 1\},\ m = 1, \ldots, M \tag{32}$$

$$\sum_{m=1}^{M} z_m^v = 1 \tag{33}$$

$$z_m^v \cdot V_{m-1} \le v_m \le z_m^v \cdot V_m,\ m = 1, \ldots, M \tag{34}$$

$$v^{\text{ch}} = \sum_{m=1}^{M} v_m \tag{35}$$

$$p_{\omega,t}^{\text{single,ch,res}} = \sum_{m=1}^{M} \left(z_m^v P_{m-1} + \frac{P_m - P_{m-1}}{V_m - V_{m-1}} \left(v_m - z_m^v V_{m-1} \right) \right). \tag{36}$$

Overall, the sizing model is expressed as a scenario-based mixed-integer linear program (MILP).

5 | CASE STUDY

The proposed model is tested on an existing Belgian end-of-life limestone quarry. In accordance with the feasibility study carried out in Section 3, we consider barrels containing 25 tons of steel slag, allowing to extract up to 1 MW of electrical power. Moreover, we estimate that at most $\bar{N}^{\text{blocks}} = 500$ blocks can be installed. The depth of the water cavity is $D = 200$ m, so that a block takes 63 seconds for a complete cycle at maximum power (descent in 22 seconds, and rise in 41 seconds). The capital costs of the UGES components are estimated in Table 1, based on industrial information. The variable maintenance and operating costs are small, that is, i.e. $MC^{\text{dis}} = MC^{\text{ch}} = 2.5$ €/MW.

The scenarios of future market prices and activation of secondary reserves are constructed based on publicly available data collected from the website of Elia,[33] the Belgian Transmission System operator. For such a long-term perspective, the accuracy of forecasting tools is questionable,[34] and the objective is rather to provide a number of time trajectories, capturing the statistical properties of the variables (daily, weekly and yearly periodicities).[35] To that end, we rely on 6 years of data (from 2012 to 2017) that are directly fed to the stochastic program, along with four artificially-generated years, in order to have a total of 10 typical years (which thus correspond to 3650 representative days). The four additional years are simply obtained by feeding the existing years into a Seasonal AutoRegressive Moving Average (SARMA) model that is used to generate new representative time trajectories.[36] The general statistical information on price scenarios are shown in Table 2. Likewise, the hourly needs in terms of upward secondary reserve for a typical week are depicted in Figure 7, where we observe the high variability of the balancing needs.

It should be noted that the scenario generation method only captures the statistical properties of historical observations, and does not model potential changes in future market conditions. To address this issue, a sensitivity analysis is performed (in Section 5.2) to properly evaluate the impact of the market variability on the UGES investment solution and the associated economic performance.

The non-linear charge and discharge curves (26), are approximated using two piecewise linear segments. The resulting MILP problem (11)-(36), with $N_\omega = 10$ scenarios composed of $N_t = 8760$ hours, is characterized by 4 029 615 constraints, 1 138 802 continuous variables, and 525 600 binary variables. It is implemented in Julia/JuMP, and solved with Gurobi 8.1.1, on a 16 GB-RAM computer clocking at 3.40 GHz.

TABLE 1 Capital expenditures (CAPEX), where the sizing variables are in gray rows and the inevitable fixed costs are in white rows

Components	Number	Costs
Geared induction machine	$\bar{n}^{\text{gm}}$	$c^{\text{gm}} = 30,000$ €
Winch	$\bar{n}^{\text{gm}}$	$c^{\text{winch}} = 500$ €
Traction cable	$\bar{n}^{\text{gm}}$	$c^{\text{cable}} = D \times (4$€/m)
Block (of 25 tons) of steel slag & flotation devices	$\bar{n}^{\text{blocks}}$	$c^{\text{blocks}} = 500$ €
Platform and mooring cables	1	5000 €
Robots (ROV)	2	2500 €/ROV
Variable frequency drive (VFD)	2	10 000 €/VFD

Price components	Mean	SD
Energy market λ^{EN}	36.6 €/MWh	23.6 €/MWh
Reserve capacity λ^{res}	6 €/MW	0 €/MW
Upward balancing market λ^{act}	40 €/MWh	4 €/MWh

TABLE 2 General information on electricity price scenarios

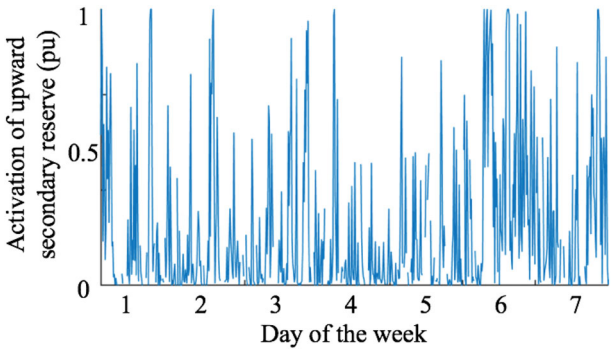

FIGURE 7 Real-time activation of upward secondary reserve during a typical week

TABLE 3 Outcomes of the investment procedure

	Arbitrage in energy market	Arbitrage in energy and reserve markets
Simulation time (min)	14	20
Number of induction machines $\bar{n}^{gm}$	1	1
Output power (MW)	1	1
Number of blocks $\bar{n}^{blocks}$	207	211
Energy capacity (MWh)	1.9	2
payback period (y)	10	9.3

5.1 | Profitability study

In what follows, we quantify the UGES profitability in two variants: (a) the profit exclusively arises from energy arbitrage, and (b) a joint participation in energy and secondary reserve markets. Firstly, Table 3 summarizes the sizing decisions, namely the number of induction machines operating in parallel (ie, the output power of the installation) and the number of blocks (ie, the UGES energy capacity). For both variants, the CPU time to solve the problem is below 20 minutes.

We see that the sizing decisions in both variants are comparable, and require investing into around 210 blocks and into a single induction machine (such that a single block can be moved at any given time), which theoretically corresponds to a storage unit of 1 MW whose maximum energy capacity (see Figure 4) is 2 MWh. Interestingly, we see that the UGES payback period can be achieved in less than 10 years (in case of perfect strategy in electricity markets). In general, UGES capital costs are estimated at around 100 €/kWh, which are lower than those of pumped-hydro energy storage (115 €/kWh), which is the current most-cost effective technology.[7] In accordance with current studies[37,38] gravity storage is expected to remain competitive to anticipated price drop of Power to Gas and Compressed Air Energy Storage systems. As a comparison, most competitive batteries are currently around 200 €/kWh, with an expected decrease down to 120 €/kWh in the coming years.[38]

To explain the attractive return on investment of UGES, we further analyze the different cash flows, that is, costs and revenues related to the optimal investment decisions (from Table 3). In particular, Figure 8 represents the annualized capital costs (Figure 8A), the repartition between revenues in energy and secondary reserve markets (Figure 8B), and the resulting annualized profits (Figure 8C), for a risk-central strategy, that is, . $r = 9\%$.

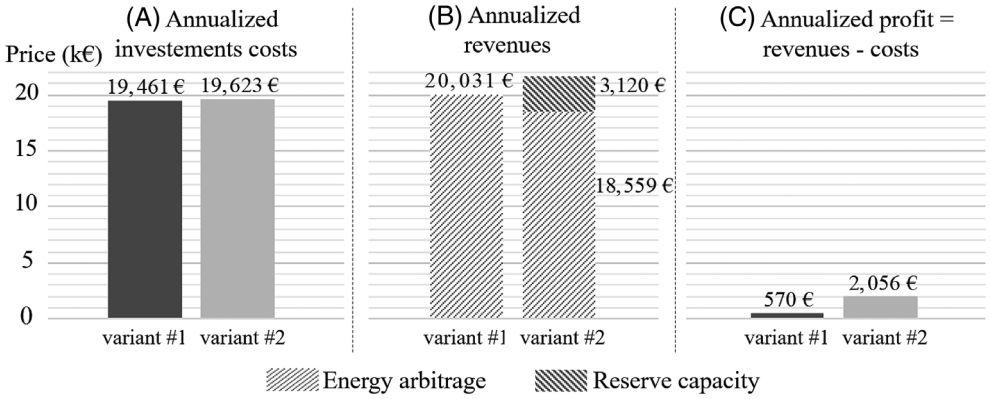

FIGURE 8 UGES costs and revenues for both studied variants

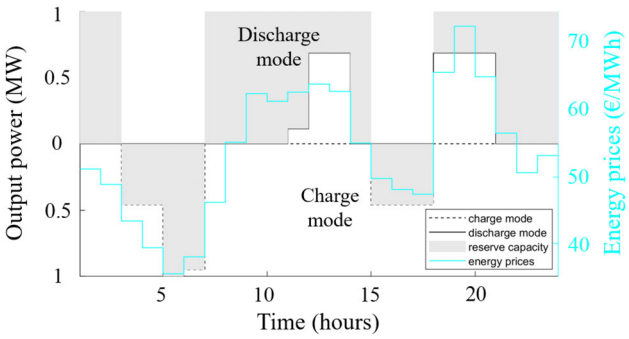

FIGURE 9 Hourly evolution of the UGES power profile over a typical day

The UGES is a profitable investment since the aggregated revenues are higher than the amortized costs. For the second (most profitable) variant combining energy arbitrage and procurement of secondary reserve, the annualized profit (annualized revenues minus the annualized CAPEX) equals to 18 559 + 3120-19 623 = 2056 €/year. The resulting return on investment (ie, the net profit divided by the investment) is 10.5%, which mainly arises by the combination of multiple advantages such as (very) low investment and operating costs, and its high flexibility allowing to stack different revenues streams.

Indeed, the procurement of reserves is an important business case for boosting the storage economic benefits.[39] The second variant results in higher profits (ie, 2056 €/year, compared to 570 for variant 1). In general, due to UGES inefficiencies, it is not profitable to trade energy when price spreads are too small. By providing secondary reserves, the storage system can still leverage profit during those hours. This effect is slightly alleviated by the need to buy more electricity from the energy market in order to compensate the real-time activation of upward reserves (revenues in the energy market of 18 559 €/year in variant 2, for 20 031 €/year when no reserves are procured in variant 1). The multi-market strategy is illustrated in Figure 9, where we analyze (for a typical day) the UGES operation profile, that is, the energy traded in the day-ahead market and the capacity offered to secondary reserves.

As expected, we see that energy is sold during peak prices, and bought during low prices. More interestingly, the unit mainly operates at intermediate power levels in discharge mode (to avoid the lower efficiency area at higher block speeds, see Figure 3). This strategy moreover allows to leave a margin for providing lucrative upward reserve capacity. When charging, the unit tends to operate at higher (more efficient) power ranges, which has also the positive effect of enabling the provision of more reserve capacity (since delivering upward reserve necessitates to decrease the power consumption).

5.2 | Robustness of the solution

It should be noted that the long lifetime of the UGES solution renders this technology very sensitive to the discount rate r (ie, inflation of investments costs and deflation of future profits). A sensitivity analysis is thus performed on the value $r = 9\%$. Indeed, this value (used as reference in the previous simulations) is a very conservative estimate that gives a

	σ_{base}	$0.5\sigma_{base}$	$2\sigma_{base}$	$4\sigma_{base}$
Simulation time (min)	1200	1072	2301	3109
Number of induction machines $\bar{n}^{gm}$	1	1	2	4
Number of blocks $\bar{n}^{blocks}$	211	210	246	277
Annualized profit (€/y)	2056	1963	6313	13 452
Return on investment [%]	10.5	10.0	23.1	33.1

TABLE 4 Results of the sizing process under different set of scenarios

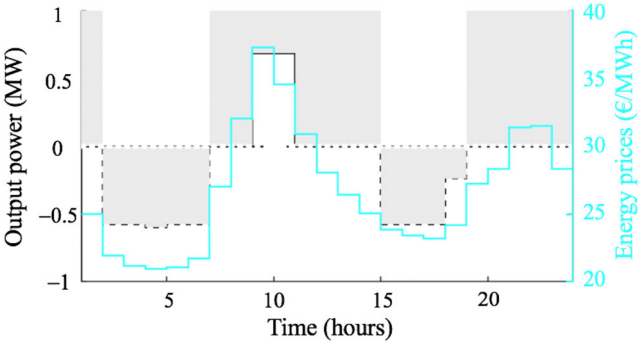

FIGURE 10 Hourly evolution of the UGES power profile over a typical day

lower bound of the profit that can be expected. With more realistic values (with respect to the current market conditions), the profitability of the UGES technology may be more attractive. In particular, a reduction of r to 6% or 4% leads to increased annualized revenues (for a joint trading in energy and reserve markets) of up to 10% and 18% respectively.

Then, it is important to study the robustness of the sizing solution in regards to the variability of future energy and reserve prices. Indeed, the initial set of scenarios is only representative of past conditions (since it is constructed using historical observations). However, the price volatility is expected to increase in the future due to the growing integration of uncertain and intermittent renewable-based generation, although this effect can be compensated by the emergence of new flexible solutions such as demand response, or other storage technologies. Our sizing process is thus performed with different sets of 10 scenarios, each one being characterized by a different variability of the market variables. Practically, we use the 10 initial scenarios, and we multiply these time series by a constant value to modify their variance. The results are summarized in Table 4, where σ_{base} is the SD associated with the initial set of scenarios.

When price fluctuations are exacerbated, it becomes profitable to rely on multiple induction machines in order to move several blocks in parallel. Indeed, price peaks are then sufficiently high and numerous so that the investment in additional power to leverage these sporadic situations is beneficial. To ensure that the energy capacity of the installation is sufficient for other hours, the number of blocks needs to be increased accordingly (eg, from 211 blocks in the reference case up to 277 in the case of extreme price volatility).

Additionally, we illustrate in Figure 10 the effects of a reduced duration of high-price period, which may be motivated by more deployment energy storage devices.

At this stage, it is important to remind that the UGES profit in the energy market is driven by price spreads, that is, differences between peak and off-peak prices, regardless of whether prices are high or low in average. In the considered day, the UGES has few opportunities in the energy market due to the smooth profile of the energy price. In particular, the energy sold to the market drops from 3.5 to 1.4 MWh (in comparison with the typical day studied in Figure 9). Interestingly, this effect is alleviated by offering more capacity in the upward reserve market. This ability to offer upward reserve when the unit is at zero-power (which occurs during most periods of the second day) is a strong advantage in comparison with pumped-storage hydro units. The latter need to be in operation to provide reserves due to their minimum power level for ensuring the stability of the hydraulic machines.[40]

Overall, these results highlight that sizing decisions can be driven by extreme scenarios, and depend thus on the risk-aversion of the investor.

6 | CONCLUSION

This paper has investigated the techno-economic viability of the innovative solution of gravity storage with solid masses, which is operating in abandoned quarry filled by water. Firstly, the system operation has been studied, and showed that, due to the water resistance, the unit's performance decreases for high-power outputs. Interestingly, the round-trip efficiency is higher than 80% when operating below two-third of the maximum installed power. Also, we observed that the UGES technology can cost-efficiently provide regulation services since transient effects infer small constraints on the unit operation, that is, reaching the maximum speed (from idle state) in a response time of 30 seconds requires an additional power of 3% with respect to the corresponding steady-state level).

At the end of the analytical study, we have derived the operating constraints of the system, which have been integrated within the sizing procedure. The methodology has then been tested on a practical case study (exploiting a typical quarry of 200 m) showing that underwater gravity storage is not only an ecological but also cost-effective solution. This is mainly due to its low investment costs, estimated at around 100 €/kWh, which are lower than rival technologies such as pumped-hydro storage or battery systems. The UGES technology is also competitive in electricity markets thanks to its ability to leverage profit from different revenue streams (by exploiting its high flexibility). In that regard, based on future scenarios of market prices, we found a payback period of less than 10 years. Importantly, we found that the solution is very robust to extreme changes in market conditions.

Overall, the UGES solution can help at cost-effectively supporting a future energy mix with more intermittent renewable generation. This work is a preliminary research in this direction, which paves the way toward more advanced studies to evaluate the technical feasibility of the proposed solution. In that regard, it is interesting to analyze the practical ability of the design to capture blocks in a reliable and timely way, as well as the resulting impact of the frequent start-ups and shut-downs on the aging of the equipment. Likewise, from an operational perspective, it is of interest to implement an advanced control scheme for ensuring a smooth continuity of supply during the transition between two blocks. Another valuable way of research regards the analysis of larger systems implemented at sea. Indeed, the largest offshore cranes can currently lift masses higher than 5000 tons, which would allow to reach an output power larger than 200 MW. Moreover, depths of several km can be exploited, which would considerably increase the energy capacity of the installation.

ORCID

Jean-François Toubeau https://orcid.org/0000-0001-9853-2694
Zacharie De Grève https://orcid.org/0000-0002-1167-7178

REFERENCES

1. Aghajani A, Kazemzadeh R, Ebrahimi A. Optimal energy storage sizing and offering strategy for the presence of wind power plant with energy storage in the electricity market. *Int Trans Electr Energy Syst*. 2018;28(11):1-16.
2. Wen X, Yu Y, Xu Z, Zhao J, Li J. Optimal distributed energy storage investment scheme for distribution network accommodating high renewable penetration. *Int Trans Electr Energy Syst*. 2019;29:1-19.
3. Barbour E, Wilson IG, Radcliffe J, Ding Y, Li Y. A review of pumped hydro energy storage development in significant international electricity markets. *Renewable Sustainable Energy Rev*. 2016;31(61):421-432.
4. Schmidt O. Levelised Cost of Storage - Gravity Storage. Imperial College Consultants and Storage Lab: 1-18; 2018.
5. Berrada A, Loudiyi K, Zorkani I. System design and economic performance of gravity energy storage. *J Clean Prod*. 2017;156:317-326. https://doi.org/10.1016/j.jclepro.2017.04.043.
6. Berrada A, Loudiyi K, Zorkani I. Sizing and economic analysis of gravity storage. *J Renewable Sustainable Energy*. 2016;8(2):1-15.
7. Zakerin B, Syri S. Electrical energy storage systems: a comparative life cycle cost analysis. *Renewable Sustainable Energy Rev*. 2015;42(C):569-596.
8. Toubeau J-F, De Grève Z, Goderniaux P, Vallée F, Bruninx K. Chance-constrained scheduling of underground pumped hydro energy storage in presence of model uncertainties. *IEEE Trans Sustainable Energy*. 2020;11:1516-1527. https://doi.org/10.1109/TSTE.2019.2929687.
9. Attarha A, Amjady N, Dehghan S, Vatani B. Adaptive robust self-scheduling for a wind producer with compressed air energy storage. *IEEE Trans. Sustainable Energy*. 2018;9(4):1659-1671.
10. EnergyVault. Ground-breaking energy storage technology enabling a planet powered by renewable resources [Online]. 2019. https://energyvault.ch/. Accessed January 2020.
11. EarthPumpStore. Gravity storage system using earth materials (EarthPumpStore) [Online]: 2019:1-4. https://www.wsset.org/docs/articles/deep-storage.pdf. Accessed January 2020.

12. Cava F, Kelly J, Peitzke W, Brown M, Sullivan S. Advanced rail energy storage: green energy storage for green energy. Trevor M. Letcher., *Storing Energy with Special Reference to Renewable Energy Sources*; Amsterdam, Netherlands: Elsevier; 2016:69-86:chap 4. https://doi.org/10.1016/B978-0-12-803440-8.00004-X.
13. Morstyn T, Chilcott M, McCulloch MD. Gravity energy storage with suspended weights for abandoned mine shafts. *Appl Energy*. 2019; 239:201-206.
14. SinkFloatSolutions. Deep ocean gravitational energy [Online]. 2019. http://sinkfloatsolutions.com. Accessed January 2020.
15. Korpas M, Holen AT. Operation planning of hydrogen storage connected to wind power operating in a power market. *IEEE Trans Energy Convers*. 2006;21(3):742-749.
16. Amjady N, Rashidi AA, Zareipour H. Stochastic security-constrained joint market clearing for energy and reserves auctions considering uncertainties of wind power producers and unreliable equipment. *Int Trans Electr Energy Syst*. 2012;23(4):451-472.
17. Nasrolahpour E, Kazempour J, Zareipour H, Rosehart WD. A bilevel model for participation of a storage system in energy and reserve markets. *IEEE Trans Sustainable Energy*. 2018;9(2):582-598.
18. ArcelorMittal. High quality ropes for mining applications. [Online]. 2015. http://ds.arcelormittal.com/wiresolutions. Accessed January 2020.
19. Al-Sharif L. Lift and escalator motor sizing with calculations & examples. *Lift Report*. 1999;52(1):1-21.
20. Munson BR, Young DF, Okiishi TH. *Fundamentals of Fluid Mechanics*. 3rd ed. Hoboken, New Jersey, United States: John Wiley & Sons; 1998.
21. ABB. HV induction motors, technical catalog for IEC motor EN 07-2016, BU motors and generators [Online]. abb.com/abblibrary/downloadcenter.
22. Ellis G. *Control System Design Guide*. 2nd ed. Cambridge, Massachusetts, United States: Academic Press; 2000.
23. Goebel C, Hesse H, Schimpe M, Jossen A, Jacobsen H. Model-based dispatch strategies for lithium-ion battery energy storage applied to pay-as-bid markets for secondary reserve. *IEEE Trans. Power Syst.* 2017;32(4):2724-2734.
24. Toubeau J-F, De Grève Z, Vallée F. Medium-term multimarket optimization for virtual power plants: a stochastic-based decision environment. *IEEE Trans. Power Syst.* 2018;33(2):1399-1410.
25. Bruninx K, Dvorkin Y, Delarue E, William D, Kirschen DS. Coupling pumped hydro energy storage with unit commitment. *IEEE Trans. Sustainable Energy*. 2015;7(2):786-796.
26. Schillemans A, De Vivero Serrano G, Bruninx K. Strategic participation of merchant energy storage in joint energy-reserve and balancing markets. Paper presented at: Mediterranean Conference on Power Generation, Transmission, Distribution and Energy Conversion (MEDPOWER 2018); November 12-15, 2018; Dubrovnik, Croatia.
27. Zou P, Chen Q, Xia Q, He G, Kang C. Evaluating the contribution of energy storages to support large-scale renewable generation in joint energy and ancillary service markets. *IEEE Trans. Sustainable Energy*. 2016;7(2):808-818.
28. Kazemi M, Zareipour H, Amjady N, Rosehart WD, Ehsan M. Operation scheduling of battery storage systems in joint energy and ancillary services markets. *IEEE Trans. Sustainable Energy*. 2017;8(4):1726-1735.
29. Pandzic H, Dvorkin Y, Carrion M. Investments in merchant energy storage: trading-off between energy and reserve markets. *Appl Energy*. 2018;230:277-286.
30. Bottieau J, Hubert L, De Grève Z, Vallée F, Toubeau J-F. Very-short-term probabilistic forecasting for a risk-aware participation in the single price imbalance settlement. *IEEE Trans. Power Syst.* 2020;35(2):1218-1230.
31. Mangasarian OL. *Nonlinear Programming*. New York: Mc- Graw-Hill; 1969, Reprint: *SIAM Classic in Applied Mathematics*. Vol 10, Philadelphia, PA; 1994.
32. Tong B, Zhai Q, Guan X. An MILP based formulation for short-term hydro generation scheduling with analysis of the linearization effects on solution feasibility. *IEEE Trans Power Syst*. 2013;28(4):3588-3599.
33. Elia Group. Elia grid data [Online]. 2019. www.elia.be/en/grid-data/data-download. Accessed January 2020.
34. Toubeau J-F, Bottieau J, Vallée F, De Grève Z. Deep learning-based multivariate probabilistic forecasting for short-term scheduling in power markets. *IEEE Trans. Power Syst.* 2019;34(2):1203-1215.
35. Klonari V, Toubeau J-F, De Grève Z, Durieux O, Lobry J, Vallée F. Probabilistic simulation framework for balanced and unbalanced low voltage networks. *Int J Electr Power Energy Syst*. 2016;82:439-451. https://doi.org/10.1016/j.ijepes.2016.03.045.
36. Toubeau JF, Hupez M, Klonari V, De Grève Z, Vallée F. Statistical load and generation modelling for long term studies of low voltage networks in presence of sparse smart metering data. Paper presented at: IECON 2016 - 42nd Annual Conference of the IEEE Industrial Electronics Society; October 23-26, 2016:3900-3905.
37. Julch V. Comparison of electricity storage options using levelized cost of storage (LCOS) method. *Appl Energy*. 2016;183:1594-1606.
38. Schmidt O, Hawkes A, Gambhir A, Staffell I. The future cost of electrical energy storage based on experience rates. *Nat Energy*. 2017;2: 17110.
39. Cho J, Kleit AN. Energy storage systems in energy and ancillary markets: a backwards induction approach. *Appl Energy*. 2014;147: 176-183.
40. Toubeau J-F, Iassinovski S, Jean E, et al. Non-linear hybrid approach for the scheduling of merchant underground pumped hydro energy storage. *IET Gener Transm Distrib*. 2019;13(21):4798-4808.

AUTHOR BIOGRAPHIES

Chloé Ponsart received the degree in civil electrical engineering in 2020 from the Faculty of Engineering of Mons, Belgium.

Zacharie De Grève received Electrical and Electronics Engineering degree in 2007 from the Faculty of Engineering of Mons, Belgium, where he received the Ph.D. degree in electrical engineering in 2012. He is currently a Researcher with the Electrical Power Engineering Unit, in the University of Mons, and a part-time Lecturer since September 2019. He conducts transverse research in machine learning, optimization and energy economics, applied to modern electricity networks with a high share of renewables, in order to contribute to the energy transition.

François Vallée received the degree in civil electrical engineering and the Ph.D. degree in electrical engineering from the Faculty of Engineering of Mons, Belgium, in 2003 and 2009, respectively. He is currently an Associate Professor with the Electrical Power Engineering Unit, Faculty of Engineering of Mons. His Ph.D. work has been awarded by the SRBE/KBVE Robert Sinave Award in 2010. His research interests include PV and wind generation modeling for electrical system reliability studies in presence of dispersed generation.

How to cite this article: Toubeau J-F, Ponsart C, Stevens C, De Grève Z, Vallée F. Sizing of underwater gravity storage with solid weights participating in electricity markets. *Int Trans Electr Energ Syst*. 2020;e12549. https://doi.org/10.1002/2050-7038.12549